ACS Catalysis

Perspective

pubs.acs.org/acscatalysis

Mesostructured Hybrid Organic–Silica Materials: Ideal Supports for Well-Defined Heterogeneous Organometallic Catalysts

Matthew P. Conley,[†] Christophe Copéret,[†,*] and Chloé Thieuleux*[,‡]

[†]ETH Zürich, Department of Chemistry and Applied Biosciences, Vladimir Prelog Weg 2, CH-8093 Zürich, Switzerland

[‡]Université de Lyon, Institut de Chimie de Lyon, UMR C2P2 CNRS-UCBL-ESCPE Lyon Equipe Chimie OrganoMétallique de Surface 43 Bvd, du 11 Novembre 1918, 69616 Villeurbanne, France

ABSTRACT: Engineering heterogeneous catalysts with molecular precision is an ongoing challenge to access materials with predictable properties that can be optimized using quantitative structure–activity relationships. One approach is grafting organometallic complexes on dehydroxylated oxide supports using surface organometallic chemistry (SOMC). Although fruitful, this technique is limited to complexes containing a σ-bound surface oxygen in the first coordination sphere of the metal. In this perspective, we describe our recent efforts to incorporate molecular diversity onto surfaces to obtain molecularly defined heterogeneous catalysts containing *N*-heterocyclic carbene ligands for C–H activation, olefin metathesis, CO_2 hydrogenation, and the *Z*-selective semihydrogenation of alkynes.

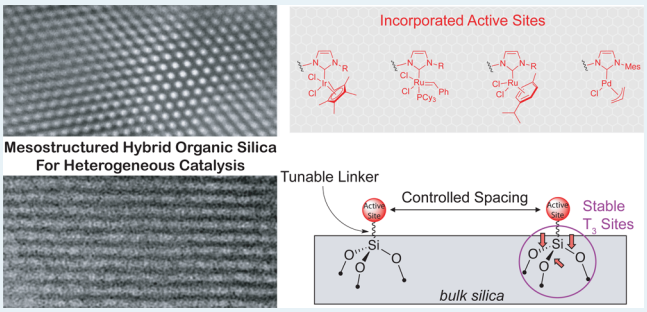

KEYWORDS: *hybrid material, heterogeneous catalysis, solid-state NMR, mesoporous silica, sol–gel, surface-enhanced NMR spectroscopy*

INTRODUCTION

Heterogeneous catalysts show key advantages in process development because they are more easily regenerated, recycled, and/or separated from reaction products.[1] For these reasons, heterogeneous catalysts dominate industrial transformations. However, most of these materials are composed of a complex mixture of surface species that are difficult to characterize, and as a consequence, the structure of their active sites is generally not understood at the molecular level. The lack of structural understanding precludes or at least impedes their rational development by establishing reliable structure–reactivity relationships and leads mainly to empirical approaches. On the other hand, homogeneous catalysts are often composed of single transition-metal centers in a defined ligand environment. Bringing molecular level definition found in homogeneous catalysis to heterogeneous materials has been a long-term research goal.[2−9]

One approach to this challenge is the generation of well-defined surface species using surface organometallic chemistry (SOMC), where the control of surface functional group density (typically an OH group) on a metal oxide surface is critical to the success of this methodology. For example, high surface area silica nanoparticles can be dehydroxylated at 700 °C ($[SiO_{2\text{-}700}]$) without significant loss of surface area and contain approximately 0.8 SiOH nm^{-1}. Protonolysis of a reactive coordination/organometallic complex by the surface silanol results in the formation of a covalent ≡Si–O–M bond (Scheme 1).[10] SOMC was extensively applied to the preparation of so-called "single-site" heterogeneous catalysts, leading to well-defined surface inorganic species with nearly every transition-metal, lanthanide, and main group element.[11,12]

Scheme 1. Grafting an Inorganic Complex on Highly Dehydroxlated Silica ($[SiO_{2\text{-}700}]$)

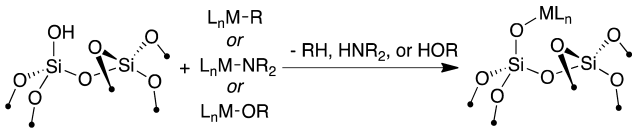

Although SOMC is successful in designing well-defined metal sites that are capable catalysts for olefin metathesis,[13−15] olefin polymerization,[2,9] and alkane homologation,[16−21] there are limitations. First, due to the amorphous structure of silica, the metal complex may graft inefficiently, or multiple grafted metal species may be present on the surface.[22] Second, the surface-bound complex must have a σ-bound oxygen ligand, e.g., siloxy, in the primary coordination sphere, which can be particularly problematic for late transition metals because the M–O bond is weak and could lead to undesired particle formation.[23] This requirement obviously limits the assortment of ligands that can be placed in the coordination sphere of the metal center, especially considering that most homogeneous catalysts are surrounded exclusively by neutral coordinating ligands (phosphines, *N*-heterocyclic carbenes, etc).

Received: December 5, 2013
Revised: March 24, 2014
Published: March 25, 2014

   dx.doi.org/10.1021/cs500262t | *ACS Catal.* 2014, 4, 1458–1469

CONTROLLED INTRODUCTION OF MOLECULAR DIVERSITY ON SILICA SURFACES

The challenge of incorporating molecular diversity on surfaces[24−26] can be addressed by designing neutral metal-binding sites onto an oxide support, in particular by selectively introducing organic functionalities onto the oxide surface. One possibility is grafting functionalized organosilane precursor onto oxide supports (Figure 1).[27−31] Though operationally simple, the

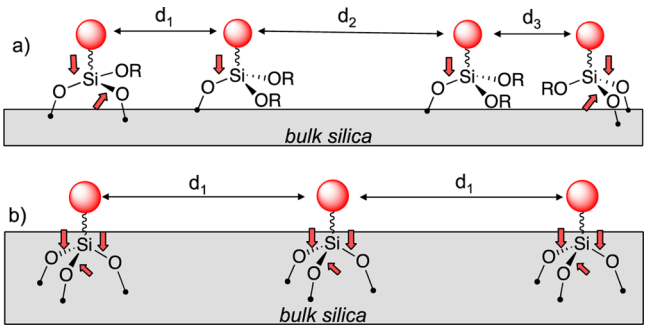

Figure 1. Schematic drawing of (a) functional silica materials prepared via surface grafting of trialkoxysilane on a silica surface; (b) hybrid organic−silica material prepared by sol−gel using a templating route. Adapted from ref 61.

distance between the organic groups is not uniform (Figure 1a), typically leading to unwanted aggregates with uneven ligand densities on the surface or even multiply ligated metal centers after coordination. Also, the silicon surface species are typically linked to the oxide support by one, possibly two, and rarely three Si−O bonds (vide infra). This variability leads to ill-defined environments around the metal center that could lead to interactions with adjacent metal sites, the support surface, and to a gradient of stability of the anchored species toward leaching.

Mesoporous hybrid materials, synthesized using sol−gel techniques in the presence of a structure-directing agent (SDA), would allow the incorporation of the organic groups (ligands) with a more regular distribution along the pore channel (homogeneous random distribution in place of patches of grafted species observed via postfunctionalization).[29,32] This methodology not only provides high surface area materials with the organic fragments on the silica inner surface pore channels but also yields materials with the organolinker attached to a silicon atom belonging to the silica matrix and typically bound by three Si−O linkages to the other silicon atoms (Figure 1b). The SDA, a molecule or a block-copolymer containing hydrophobic and hydrophilic units, self-assembles into micelles under controlled experimental conditions (temperature, concentration, pH, etc.) and provides a template for the formation of porous oxide materials.[33]

Although the mechanisms involved in the formation of pure mesoporous silica/oxide frameworks are well-established, the exact mechanism and parameters controlling the incorporation of organic ligands remain unclear. Nonetheless, the more regular distribution probably arises from constructive supramolecular interactions between the hydrophobic organic fragment of the organosilane precursor and the hydrophobic core of the SDA micelle, as well as possible interactions between the polar Si−OH groups of the organosilane and the SDA hydrophilic head during hydrolysis and silica condensation. One can propose that the free energy minimization of the thermodynamically stable micellar structure imposes the random distribution of hydrolyzed organosilanes, R−Si(OH)$_3$, within the micelle, hence the more regular (random) distribution of these moieties. After material synthesis, the SDA is removed from the silica mesopores by Soxhlet extraction, which can leave residual amounts of SDA in the micropores. Washing the material in pyridine, water, and dilute HCl buffer quantitatively removes the SDA from the mesopores and micropores.[34] The characterization of the SDA free materials by ^{29}Si solid-state NMR confirms the presence of mostly tripodal silicon surface species bearing the organic group (T_3 sites), with minor amounts of T_2 sites, which is in contrast to postsynthetically modified silica that generally contains strong T_1 as well as T_2 site spectral signatures.[35]

The regular distribution of the organic groups within the silica matrix is usually inferred by chemical reactivity.[36−38] Recently, we probed site homogeneity using EPR spectroscopy for materials containing TEMPO radicals installed in the pore channels. These materials were synthesized starting from **Mat-Azide** (**1**),[39] which were reduced to the amine materials **Mat-NH$_2$** (**2**) under Staudinger conditions (Figure 2).[40] The reaction is very clean on the surface, and the only byproduct is unreacted azide (10−30%),

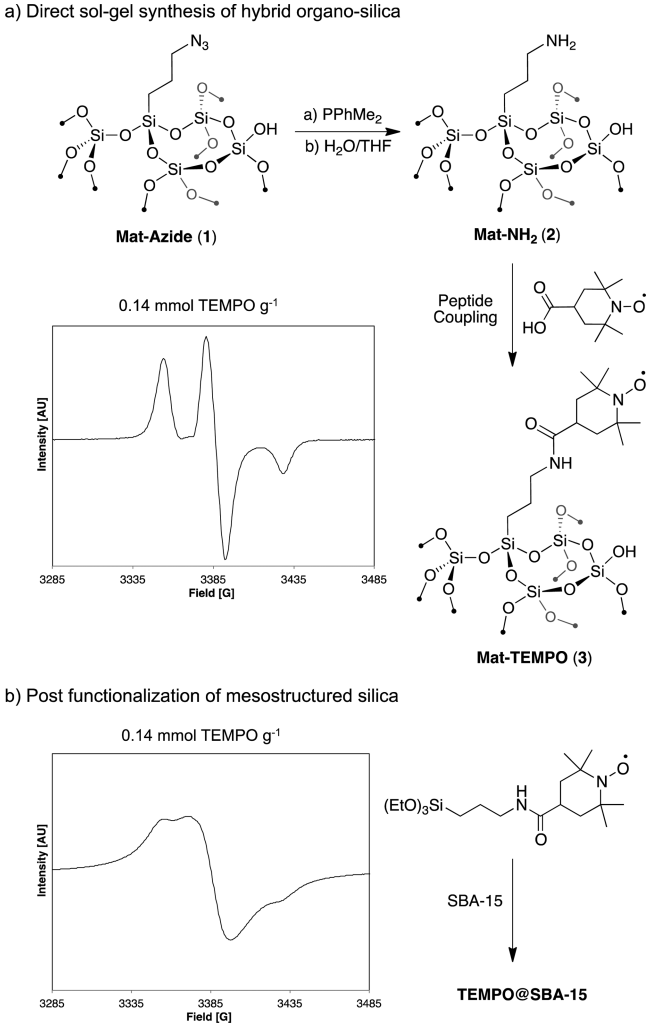

Figure 2. (a) Synthesis of **Mat-NH$_2$** (**2**) and **Mat-TEMPO** (**3**) materials from **Mat-Azide** (**1**) and the EPR spectrum of **3** at 0.14 mmol g^{-1} TEMPO. (b) TEMPO@SBA-15 prepared by postsynthetic modification of SBA-15 and the EPR spectrum of 0.14 mmol TEMPO g^{-1}.

dx.doi.org/10.1021/cs500262t | ACS Catal. 2014, 4, 1458−1469

Scheme 2. Synthesis of Imidazolium-Containing Hybrid Materials Using Three Strategies: (a) Nucleophilic Displacement of a Halide Using Mesitylimidazole; (b) Conversion of 1 to 7 by Condensation of 2 with Arylamines, Glyoxal, and Formaldehyde; (c) Direct Sol–Gel Synthesis of 8

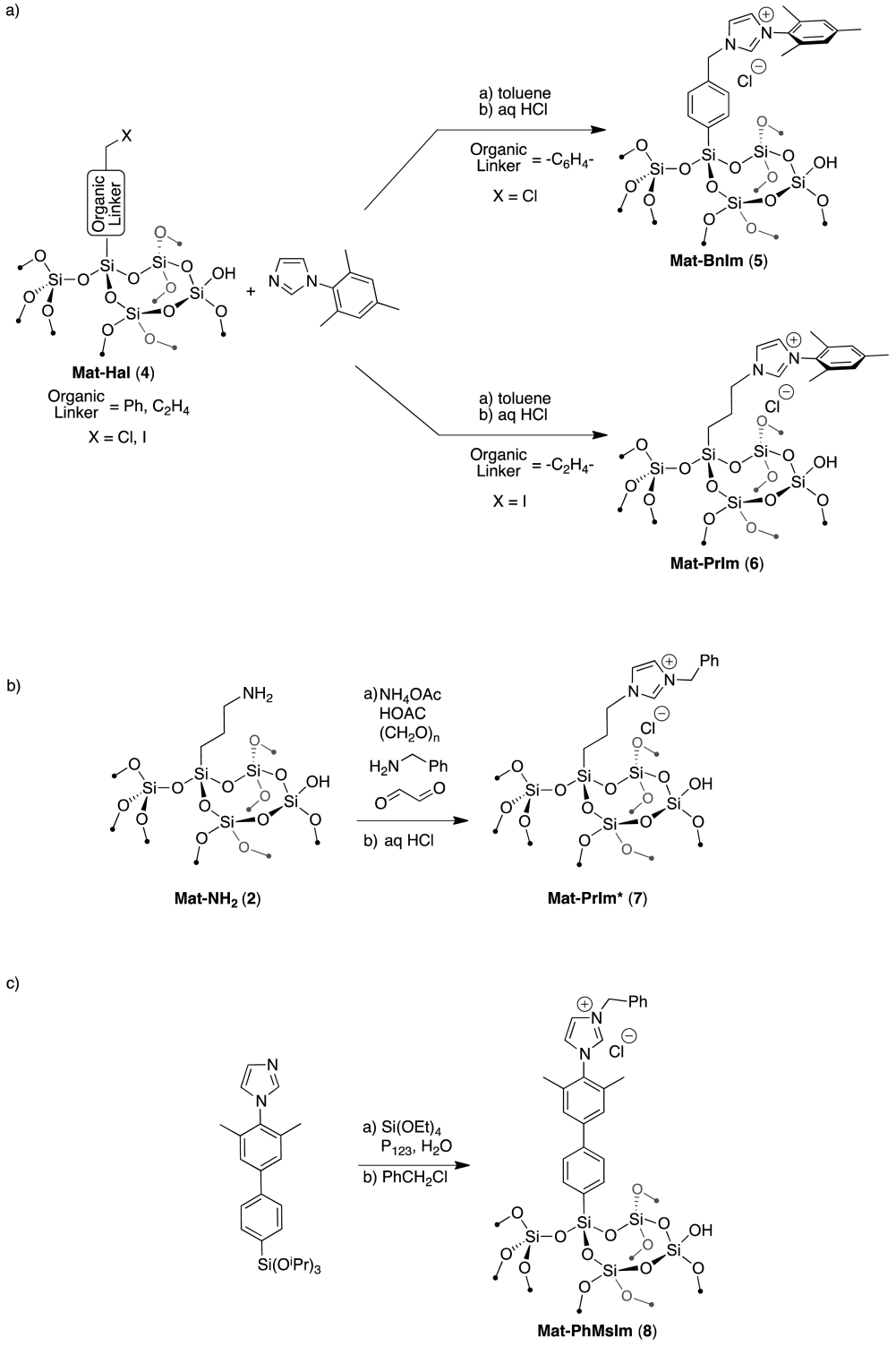

as confirmed by solid-state NMR analysis.[40] Using benzotriazole-mediated coupling of **2** and 4-carboxy-TEMPO, we generated a library of **Mat-TEMPO** (**3**) materials with 0.010–0.28 mmol TEMPO g^{-1} material.[41] The amount of radical was dependent on the initial TEOS/3-azidopropyltrimethoxysilane ratio used in the sol–gel synthesis of **1** (Figure 2a).

The EPR line width is directly associated with the dipolar coupling between two radicals, and it scales with r^{-3}. At the same TEMPO loadings (0.14 mmol TEMPO g^{-1}), **3** has a line width of 15 G while SBA-15 containing TEMPO prepared by postsynthetic modification[42−46] has a much broader EPR line shape (27 G, Figure 2). The much larger EPR line width

dx.doi.org/10.1021/cs500262t | ACS Catal. 2014, 4, 1458–1469

observed for the SBA-15 material postfunctionalized with TEMPO clearly indicates a very broad distribution of radical−radical distances with many of them in close proximity. In fact, the EPR spectrum of this postsynthetically modified material has a significantly larger line width than even the highest concentration **3** (0.28 mmol TEMPO g^{-1}, 21 G) accessible by sol−gel techniques in the presence of SDA. The EPR spectra of **Mat-TEMPO** materials can be modeled using a simple pair distribution analysis,[39] which established that the TEMPO fragments are distributed randomly in the mesopores in a narrow distribution of inter-radical distances in contrast to patches of radicals as observed by postgrafting approach of organo-(trialkoxy)silane, R−Si(OR′)$_3$, on mesostructured silica materials. These results indicate that the materials prepared by sol−gel templating routes have desirable properties similar to the ideal design principles outlined above.

Hybrid materials have a rich history as acid and/or base catalysts for various organic reactions, and in some cases, they exhibit beneficial cooperative properties.[47−53] Transition-metal catalysts anchored to solids are typically prepared using postsynthetic modification,[31] and only a few articles deal with the preparation of supported transition metal complexes using the template-mediated route, mainly dealing with coordination compounds.[54,55] One notable example in organometallic systems is the heterogenized Grubbs−Hoveyda-type complexes that were successfully supported via the alkylidene ligand in the pores of a HMS type silica for diene and enyne ring-closing metatheses.[56,57] We constructed materials that contained imidazolium units in the mesopores of the silica, because this organic group can lead to the formation of *N*-heterocyclic carbene metal complexes (NHC−M) that are ubiquitous in catalysis.[58,59] These NHC-containing materials were obtained using the three strategies shown in Scheme 2. In all cases, tetraethoxyorthosilicate (TEOS) was mixed with varying amounts of a functional organotri(alkoxy)silane in the presence of the block copolymer Pluronic P123 as SDA. In Scheme 2a, the alkylhalide containing material **Mat-Hal** (**4**)[60] was reacted with mesitylimidazole to yield either **Mat-PrIm** (**5**) or **Mat-BnIm** (**6**).[61,62] The nucleophilic substitution of the terminal halogeno group on alkyl/benzyl chain with the imidazole generates **5** and **6** in near quantitative yields. These starting materials are very versatile, easy to prepare, and several loadings of halogeno moieties are readily accessible.[60] Another strategy is shown in Scheme 2b and involves treatment of **2** with glyoxal, NH_4OAc, and an amine to yield the imidazolium-containing solid **7**. This reaction is very clean from solid-state NMR analysis, with the only byproduct being unreacted azide from the Staudinger reduction.[40]

We have also reported materials that contain very rigid linkers between the silica surface and the imidazolium (**Mat-PhMsIm** (**8**)) by the co-condensation of the imidazole−triethoxysilane and TEOS followed by reaction with an alkyl halide (Scheme 2c).[63] These three strategies yield materials that have physical properties (2D-hexagonal or wormlike structures, high BET surface area, large pore volume, Figure 3) similar to those of the parent hybrid−silica materials, indicating that the physical characteristics of the material are preserved during these chemical transformations. Additionally, these materials were characterized by solid-state NMR spectroscopy that confirmed the molecular level structure of the imidazolium fragment on the surface.

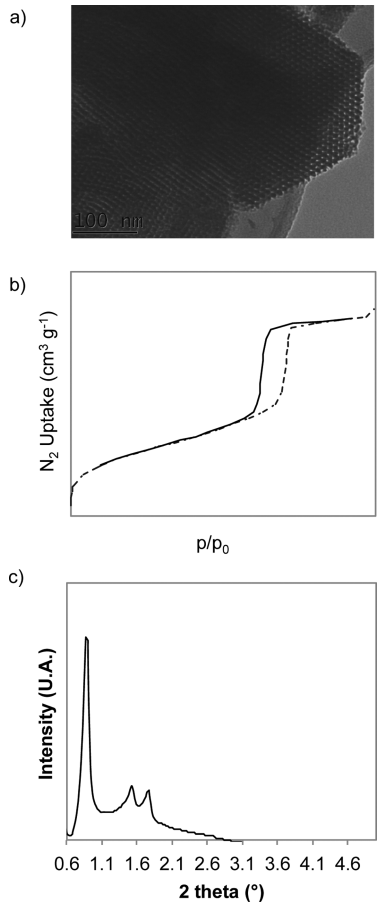

Figure 3. Representative (a) TEM micrograph, (b) N_2 adsorption−desorption isotherm, and (c) X-ray diffraction pattern for **8**.

SELECTIVE METAL COMPLEX FORMATION ON FUNCTIONALIZED SILICA SURFACES

The silica surface of these engineered hybrid materials contains two sites that can bind the transition metal, the imidazolium and surface silanols. Selective activation of the imidazolium salt to generate a free carbene or an appropriate transmetalation reagent to form the desired NHC−M complex could be complicated by side reactions with surface silanols. Selective activation of the imidazolium was addressed by passivation of the surface silanols with methanol, to form ≡Si-OMe, or with trimethylsilyl halides, to generate unreactive ≡Si-OSi$(CH_3)_3$ surface species that tolerate the reagents necessary to form the NHC−M sites. The consumption of isolated silanols is evidenced by infrared spectroscopy. Depending on the metal complex, a careful choice of the passivation agent is necessary. For example, we reported **Mat-Ir** (**10**),[61] a mesostructured hybrid silica material that contained NHC−Ir fragments within the material. In this case, we synthesized **Mat-Ag** (**9**) containing materials from AgOC-$(CF_3)_3$, a soluble Ag(I) source,[64] that are ideal for transmetalation to iridium complexes to ultimately form **10** (Scheme 3). The metal precursor, $[Cp^*IrCl_2]_2$, is quite robust and is selective to the reaction with the NHC−Ag species on the surface. We found that surface silanol passivation with either methanol or trimethylsilyl halides is sufficient to yield **10**.

Silver transmetalation is unfortunately not compatible with the formation of most NHC−Ru metathesis catalysts, typically leading to a complex reaction mixture. Strong bases were

dx.doi.org/10.1021/cs500262t | *ACS Catal.* 2014, 4, 1458−1469

Scheme 3. Synthesis of Surface NHC−M Complexes. (a) Route A Using Intermediate NHC−Ag Species to Access 10. (b) Examples of Functionalized Materials with Organometallic Fragments Accessible through Route B

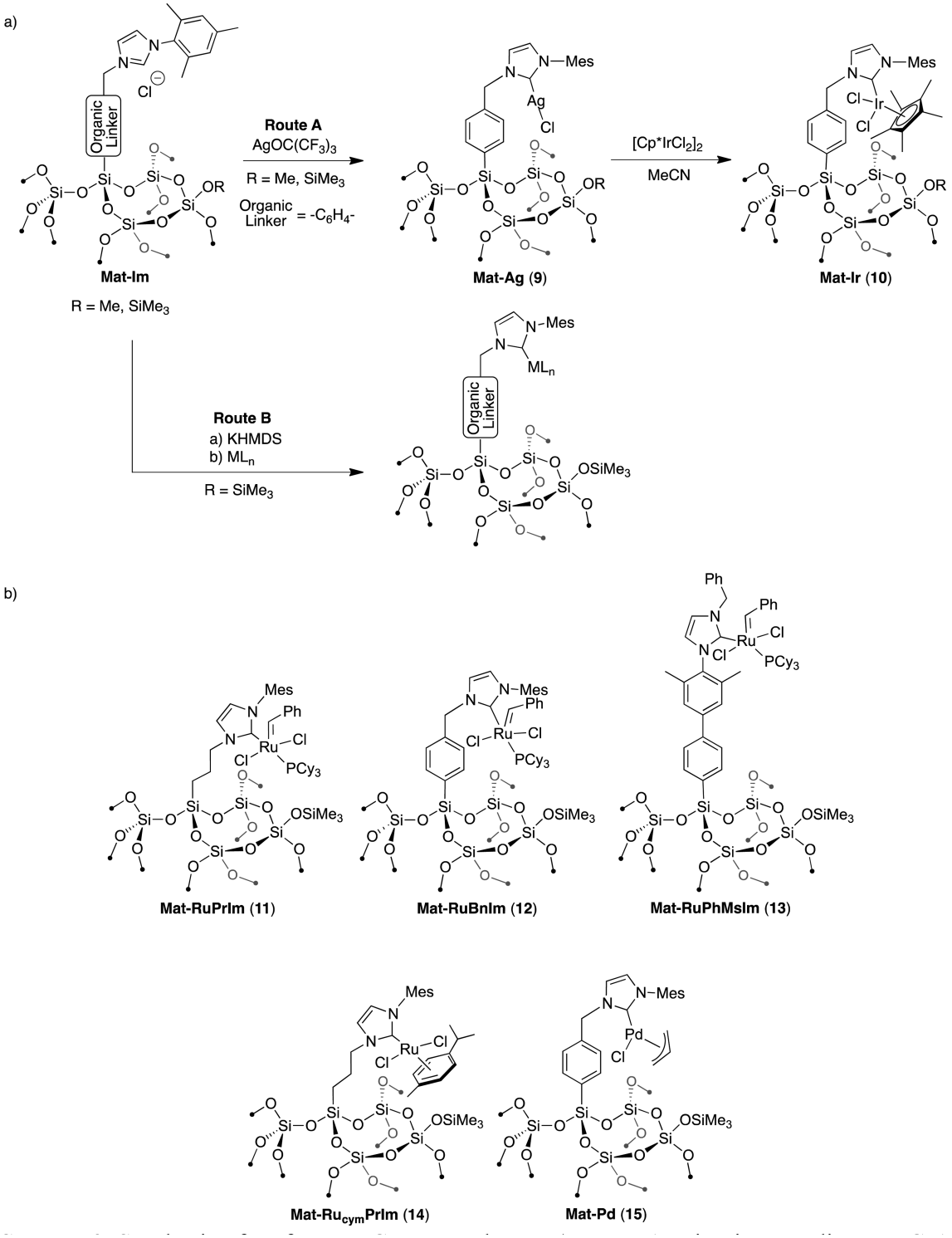

explored in attempts to generate the free NHC in situ, and only materials passivated with ≡Si-OSiMe$_3$ groups are compatible with these reaction conditions. Contacting **5**, **6**, or **8** with KHMDS, followed by trapping with [Cl$_2$Ru(=CHPh)(PCy$_3$)$_2$], gave **Mat-RuPrIm** (**11**) or **Mat-RuBnIm** (**12**) in ca. 20% yield and **Mat-RuPhMsIm** (**13**) in ca. 40% yield, based on Ru elemental analysis (Scheme 3b).[62] This strategy is quite general and has been applied to **Mat-Ru$_{cym}$PrIm** (**14**, 60% yield from Ru elemental analysis)[65] and **Mat-Pd** (**15**, 85% yield from Pd elemental analysis).[66]

INDIRECT CHARACTERIZATION OF METAL-CONTAINING MATERIALS FROM REACTIVITY PATTERNS

We determined the nature of metathesis active sites in **11** and **12** using ethyl oleate as a model reactant by determining the *E*/*Z*

dx.doi.org/10.1021/cs500262t | ACS Catal. 2014, 4, 1458−1469

Scheme 4. (a) Metathesis of Ethyl Oleate. (b) Four of the Possible Eight Approaches (Alkylidene Substituent = R^1 or R^2; Here R^1 Was Chosen) of a Dissymmetric *Z*-Olefin to a Ruthenium Alkylidene with the Corresponding Metallocyclobutanes and Metathesis Products from Each of the Four Species

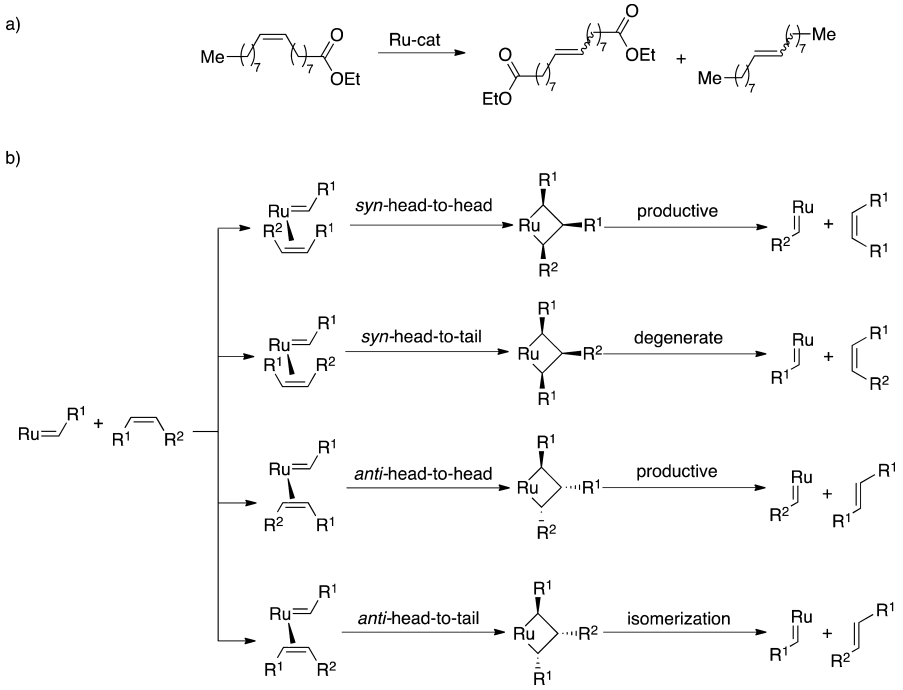

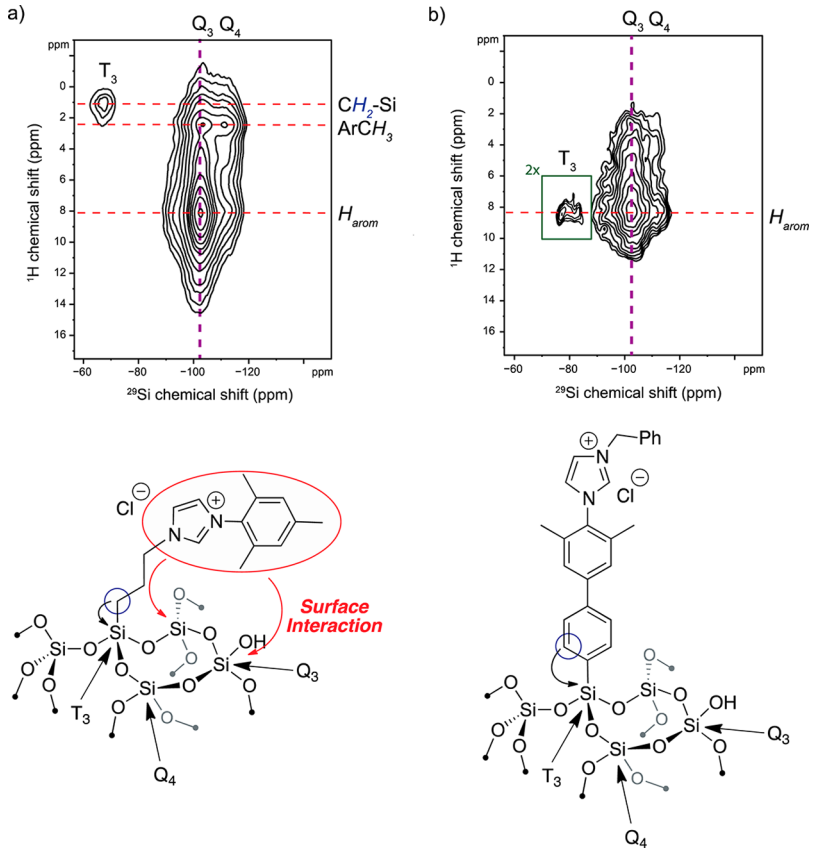

Figure 4. (a) $^1H-^{29}Si$ HETCOR spectrum of **6**. (b) $^1H-^{29}Si$ HETCOR spectrum of **8**. The stucture of each material is shown below the respective spectrum (adapted from ref).

products selectivity at low conversions (Scheme 4a).[62,67,68] The *E*/*Z* ratio depends on the approach of the alkene toward the alkylidene, and in Scheme 4b, the different possible olefin approaches are shown. The *Z*-alkene can approach the alkylidene

dx.doi.org/10.1021/cs500262t | *ACS Catal.* 2014, 4, 1458−1469

in a *syn*/*anti* as well as head/tail fashion leading to four possible metallocyclobutanes. The *syn*-head-to-head and *anti*-head-to-head approach will give productive metathesis, *anti*-head-to-tail will isomerize the olefin, and *syn*-head-to-tail will result in a degenerative process. The *E*/*Z* ratio will be determined by the nature of the active site that will in turn be sensitive to subtle variations in the ligand architecture around the ruthenium center. Because the *anti*-head-to-tail intermediate results in isomerization, extrapolation of the *E*/*Z* product ratio at 0% conversion provides the intrinsic selectivity of the active sites.

We determined the *E*/*Z* ratio for several homogeneous Ru catalysts and found that there are large differences in *E*/*Z* ratio between Cy_3P−Ru (Grubbs-I generation) and NHC−Ru (Grubbs-II generation) complexes. Cy_3P−Ru catalysts give *E*/*Z* ratios of 3.5−3.6 for 9-octadecene metathesis products, whereas ratios ranging from 2.3−2.6 were obtained for NHC−Ru complexes. The substituents on the NHC ligands have little effect on *E*/*Z* ratio. Both **11** and **12** have extrapolated *E*/*Z* ratios around 2, close to the *E*/*Z* ratio obtained from the corresponding molecular NHC−Ru complexes. This result indicates that NHC−Ru sites are responsible for catalysis in these mesostructured materials. Finally, there is a small but significant difference in the *E*/*Z* ratios of **11** (2.0) and **12** (2.2) for 9-octacedene metathesis products at steady state, suggesting that the more flexible linker may promote surface interactions with ruthenium, which would favor reaction pathways where the Ru−carbene and the *cis*-olefin point away from the surface.

SPECTROSCOPIC CHARACTERIZATION OF METAL-CONTAINING MATERIALS

The detailed characterization of these well-defined heterogeneous catalysts is necessary to confirm the surface structures of the materials. Small-angle X-ray diffraction, TEM, and N_2 absorption indicate that these materials maintain their bulk properties. We routinely employ solid-state NMR spectroscopy and compare the NMR spectra of the material with a closely related homogeneous precursor that generally allows complete structural assignment. For example, the ^{13}C cross polarization magic angle spinning (CPMAS) NMR spectrum of **10** contains key aromatic resonances that are in good agreement with a structurally related homogeneous NHC−Ir complex. However, the dilution of NHC−Ir in the material requires extensive experiment acquisition time to obtain 1D ^{13}C NMR spectra with good signal-to-noise ratio. In fact, observing the key NHC−Ir resonance requires isotopic enrichment at the C(2) position of the imidazolium moiety. The ^{13}C CPMAS of isotopically enriched **10** contains a signal at 176 ppm, which is in excellent agreement with the chemical shift C(2)Ir−C bond in homogeneous model complexes.[61] Solid-state NMR has also been applied to establish the structure of **14**[65] and **15**[66] (vide infra).

IS THE SURFACE INNOCENT? CONFORMATIONAL ANALYSIS FROM NMR STUDIES

Though the presence or absence of surface interactions affecting catalysis in these materials is an intriguing hypothesis, such surface metal interactions are difficult to characterize directly using available spectroscopic methods. Only heteronuclear solid-state NMR spectroscopy could determine the conformation of the NHC−Ru fragment on the silica surface. As mentioned for **10**, the low functional group density present in this material renders this technique too time-consuming for nonisotopically enriched materials.

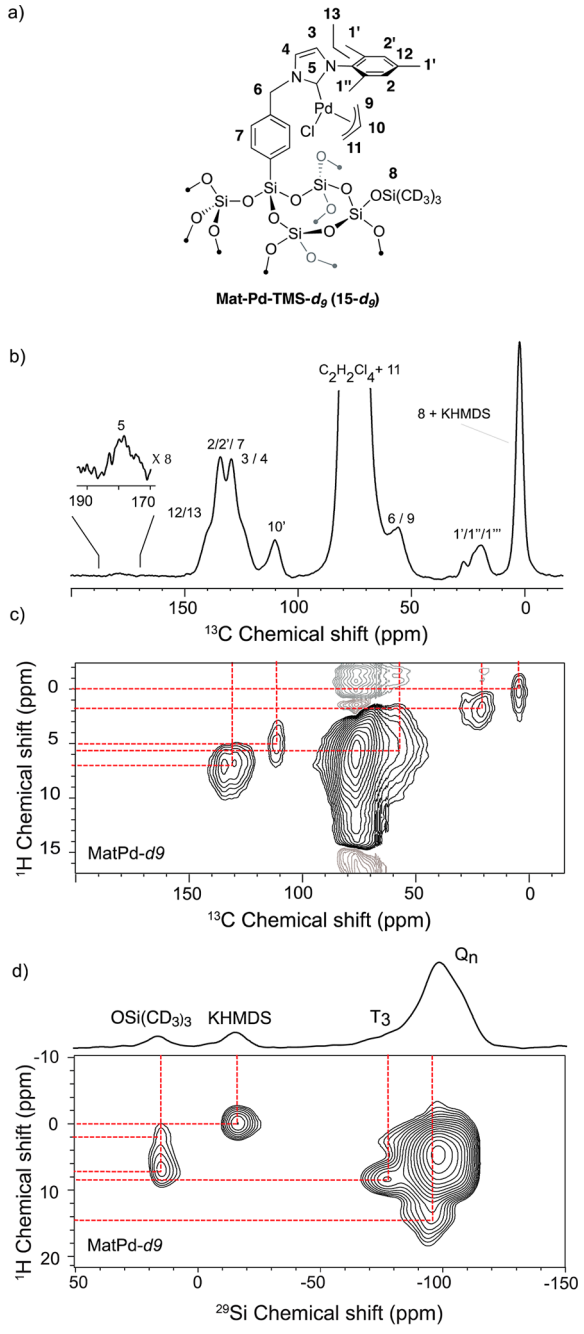

Figure 5. DNP SENS spectrum of **15**-d_9. (a) Structure of **15**-d_9 with labeling, (b) ^{13}C CPMAS, (c) ^1H−^{13}C HETCOR, and (d) ^1H−^{29}Si HETCOR spectrum of **15**-d_9.

We recently found that fast NMR characterization of these materials could be achieved with dynamic nuclear polarization surface-enhanced NMR spectroscopy (DNP SENS),[69] which provides up to a factor of ca. 250 NMR signal enhancements for surface species.[35,70−74] In DNP SENS, a permanent radical polarizing agent is introduced by incipient wetness impregnation of the material in a suitable solvent. Microwave irradiation of the EPR transition at low temperature (∼100 K) yields ^1H DNP enhancements of the frozen solid. Cross polarization can then be used to transfer the enhanced ^1H magnetization selectively to the heteronuclei present on the material surface.

We compared the surface interactions in flexible **11** and rigid **13** using DNP SENS.[63] Wetting either material with a 12 mM

dx.doi.org/10.1021/cs500262t | *ACS Catal.* 2014, 4, 1458−1469

Scheme 5. H/D Exchange Reaction of Acetophenone Catalyzed by 10 or 16, the Homogeneous Equivalent

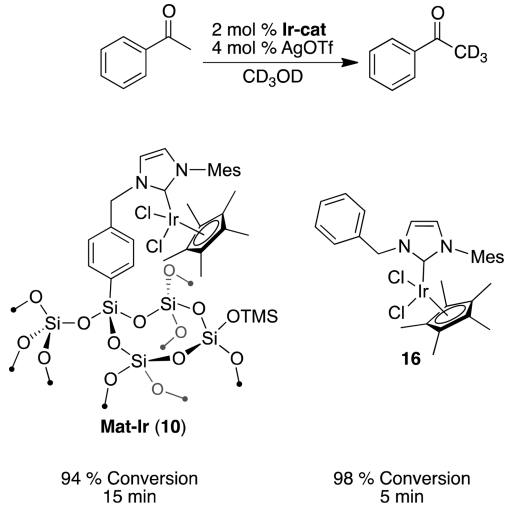

solution of aqueous TOTAPOL,[75] a common polarizing agent, gave sufficient signal enhancements to acquire $^{1}H-^{29}Si$ HETCOR spectra in only a few hours. The solid-state HETCOR experiment determines the proximity of a pair of nuclei through space (dipolar interactions).[76,77] These spectra for **6** and **8** contain the expected interactions between the T-sites and the nearest protons (aliphatic for **6** and aromatic for **8**). The $^{1}H-^{29}Si$ HETCOR spectrum of **6** also contains strong correlations between the methyl protons from the mesityl groups and bulk silica Q_4 sites (Figure 4a), similar correlations between aromatic methyls and bulk silica signals are absent in **8** (Figure 4b). This result indicates that the flexible propyl chain folds the imidazolium onto the silica and would promote interactions between the ruthenium and surface siloxane bridges, which is not possible with the rigid linker. These spectroscopically evidenced surface interactions play a large role in olefin metathesis catalysis; the flexible-surface-interacting **11** is a much more stable and active catalyst than the rigid **13**.

Mat-Pd-TMS-d_9 (**15-d_9**, Figure 5a), **15** passivated with TMS-d_9 groups,[78] contains a supported NHC−Pd π-allyl complex for the semihydrogenation of alkynes and was fully characterized by DNP SENS in very short experiment times by incipient wetness impregnation of a 1,1,2,2-tetrachloroethane[38] solution of a bulky polarizing agent bCtbK.[40,79] We should note that this is the first example of DNP SENS application to an organometallic complex supported on a hybrid material, and we show that this NMR method is applicable to metal-containing functional materials. The ^{13}C CPMAS NMR spectrum contained the key NHC−Pd carbon with only 35 min of NMR experiment acquisition at natural isotopic abundance (Figure 5b), the first time this particular resonance has been observed in these materials without isotopic enrichment. Each assignment was confirmed with a $^{1}H-^{13}C$ HETCOR solid-state NMR experiment (Figure 5c). The semiflexible linker present in this material led us to carefully scrutinize the conformation of the NHC−Pd fragment with respect to the surface. Indeed, we found that the methyl groups from the mesityl ring are interacting with bulk silica signals in the $^{1}H-^{29}Si$ HETCOR spectrum (Figure 5d), suggesting that surface interactions could be a general phenomenon for materials that have flexible linkers.

CATALYTIC APPLICATIONS OF SINGLE-SITE HYBRID MATERIALS

Each of the materials was designed as a catalyst for different applications. Both **11** and **12** are heterogeneous variants of a Grubbs-II catalyst, **10** was modeled from homogeneous NHC−Ir catalysts for the H/D exchange of aromatic ketones, **14** is an efficient CO_2 hydrogenation catalyst, and **15** catalyzes the *Z*-selective semihydrogenation of alkynes. We will briefly discuss the catalytic properties of these materials below.

Alkene Metathesis.[62] We observed that **11** catalyzes the metathesis of ethyl oleate at low loadings (ca. 0.01%) in 5 h at 40 °C with an initial rate of 65 min^{-1}, whereas **12** also catalyzed ethyl oleate metathesis with similar performances, though with a slightly lower TOF of 30 min^{-1}. Lower loadings of **11** (0.003 mol %) efficiently convert ethyl oleate to its thermodynamic mixture in about 24 h, corresponding to a minimum turnover number of 17 000 mol ethyl oleate (mol Ru)$^{-1}$. In all cases, no detectable amount of ruthenium leaching was observed in the reaction mixtures from ICP analysis, and these catalysts can be recycled up to seven times without loss of activity.

Catalytic H/D Exchange.[61] Catalytic tests of **10** activated with AgOTf in the iridium-catalyzed H/D exchange of acetophenone[80,81] established that this material was an active catalyst (Scheme 5). In a typical experiment, acetophenone was dissolved in methanol-d_4 in the presence of 2 mol % **10**. Most of the acetophenone (94%) was converted to acetophenone-d_3 within 15 min. Recycling experiments of **10** resulted in minimal rate and yield decreases after three catalytic cycles. Under these conditions, the analogous homogeneous complex **16** has similar catalytic behavior as **10**.

We investigated the **Mat-Ir**-catalyzed H/D exchange in different pore size materials.[82] These mesostructured materials present similar physical features (2D hexagonal, surface area, pore volumes) except the size of the average mesopore diameters (3 vs 6 nm calculated using the Barrett−Joyner−Halenda (BJH) method from the adsorption branch of the N_2 adsorption/desorption isotherm). We also varied the substituents on the NHC fragment to determine if either the pore size of the material or the substitution pattern of the NHC fragment have an impact on the overall reaction kinetics in the **Mat-Ir** catalyzed H/D exchange reaction. The structures of the catalysts investigated are shown in Scheme 6. The NMR spectral properties of these two families of materials establish that both have nearly identical NHC−Ir molecular environments. Though these materials have very different pore sizes, the dominating influences on catalytic activity are the substituents on the NHC fragment, as has been thoroughly documented in homogeneous catalysis. For example, the large ketone 9-acetylanthracene is near fully converted to the product with similar rates if homogeneous **16** or heterogeneous **MeNHC-Ir** with either a 3 nm or 6 nm pore size are used as catalysts (Table 1, entry 2).

CO_2 Hydrogenation.[65] The use of carbon dioxide as a C_1 building block offers obvious economic and environmental advantages. Ruthenium-catalyzed conversion of CO_2 into formic acid,[83] formates,[84,85] and formamides[86] is known, though heterogeneous variants are relatively unexplored.[87,88] The hydrogenation of CO_2 is catalyzed by **14**. During NMR characterization, we discovered that reversible coordination of THF and dissociation of the *p*-cymene fragment from the ruthenium center takes place during the synthesis of **14** (Scheme 7).

dx.doi.org/10.1021/cs500262t | ACS Catal. 2014, 4, 1458−1469

Scheme 6. Catalysts Used for the Ir-Catalyzed H/D Exchange

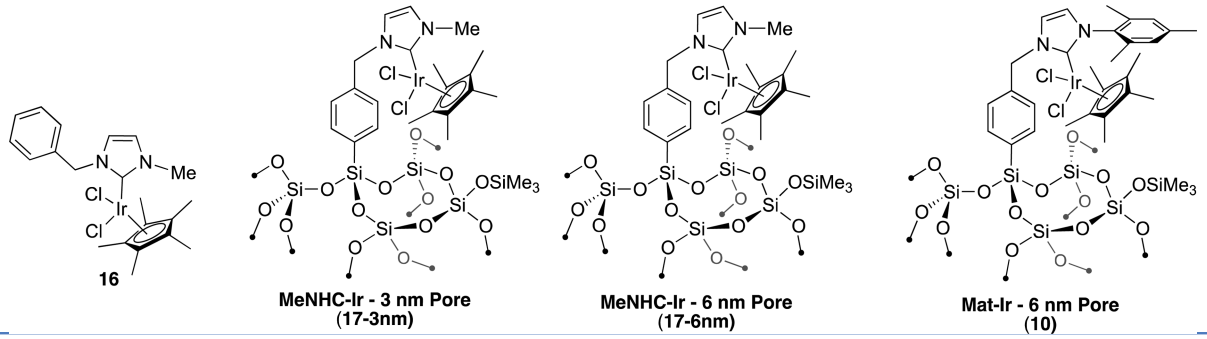

Table 1. H/D Exchange Catalyzed by 15, 16, MeNHC-Ir (3 nm Pore, 17-3 nm), MeNHC-Ir (6 nm Pore, 17-6 nm) or 10 (6 nm Pore) with Different Pore Sizes or NHC Substituents at 100 °C

Entry	Substrate	15	16	17-3nm	17-6nm	10
1		99[a]	-	95	94	95
		[5 min][b]		[15 min]	[15 min]	[15 min]
2	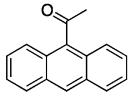	90	97	97	92	96
		[5 min]	[25 min]	[25 min]	[25 min]	[35 min]
3	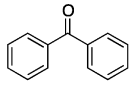	60	59	28	28	-
		[12 h]	[12 h]	[12 h]	[12 h]	
4		27	39	27	32	-
		[12 h]	[12 h]	[12 h]	[12 h]	

Scheme 7. Reversible Coordination of THF to 14 and Synthesis of 18

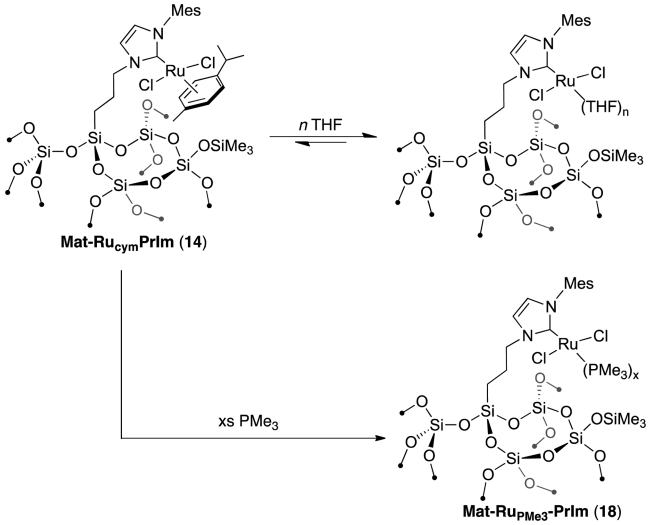

In the presence of 5300 equiv of pyrrolidine per ruthenium under 50 bar CO_2 and 30 bar H_2, **14** catalyzes the conversion of carbon dioxide to 1-formylpyrrolidine (Scheme 8). However, this catalyst is unstable under the reaction conditions (TON = 260), as observed for the homogeneous complex **19**. Because most active Ru-based CO_2 hydrogenation catalysts contain strong σ-donor phosphine ligands,[86,89] **14** was contacted with PMe_3 to give the **Mat-Ru$_{PMe3}$-PrIm** (**18**) material, which was also characterized by multinuclear solid-state NMR spectroscopy. This modification of the active site lead to improved catalyst stability allowing 2900 TON to be reached.

Z-Selective Hydrogenation of Alkynes.[66] The *Z*-selective semihydrogenation of alkynes was investigated with catalytic amounts of **15**. The *Z*-selective semihydrogenation of alkynes (**Yne**) can yield three products: the desired *Z*-alkene (**Z-Ene**), the unwanted *E*-alkene isomer (***E*-Ene**), or the over-reduced alkane product as shown in Scheme 9. In the presence of dihydrogen, **15** is active in semihydrogenation of 1-phenylpropyne (**Yne-1**) with a turnover frequency (TOF) of 1800 h^{-1} and 93% selective toward ***Z*-Ene-1**. A high turnover number (TON = 1100) was obtained for this substrate, though at higher substrate/catalyst ratios, it did not lead to full alkyne conversion indicating that the catalyst deactivates. Palladium does not leach into solution during catalysis as verified by less than 1 ppm Pd in the product mixtures from ICP analysis.[90,91] Finally, the formation of the alkane byproduct occurs only at high alkyne conversion (>90%), and at >99% **Yne-1** conversion, only a slight decrease in selectivity was observed. Under similar conditions, the homogeneous analogue, **20**, transforms **Yne-1** to **Z-Ene-1** with 90% selectivity at 50% conversion, though the catalyst is less stable (TON ca. 100) and the selectivity drops precipitously at >90% conversion with the alkane as the major byproduct. Related NHC−Pd(0) complexes have a TOF of about 45 h^{-1} in **Yne-1** semihydrogenation with a selectivity of 75% for the *Z*-alkene at 99% conversion.[92] These results indicate that **15** is much more active and selective than closely related homogeneous NHC−Pd complexes.

The scope of the **15**-catalyzed semihydrogenation of alkynes is shown in Scheme 9 and illustrates that **15** efficiently reduces diphenylacetylene **Yne-2** with 81% selectivity at 50% alkyne

dx.doi.org/10.1021/cs500262t | ACS Catal. 2014, 4, 1458−1469

Scheme 8. Hydrogenation of CO_2 (50 bar) in the Presence of H_2 (30 bar) and Pyrrolidine Catalyzed by 19, $RuCl_2(PMe_3)_4$, 14, and 18

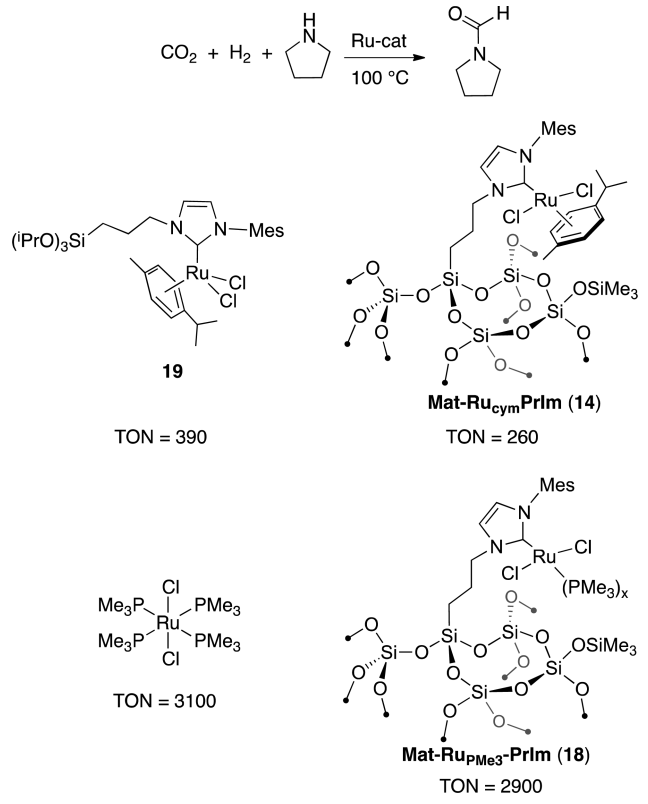

conversion and 56% at >99% conversion. Furthermore, 1-octyne gives 1-octene with good selectivity at low conversion; however at high alkyne conversion (>70%) C_{16} byproducts are formed that reduce the yield of 1-octene. In addition, **15** cleanly semihydrogenates internal alkyl alkynes with good activity and selectivity and even tolerates primary alcohol functionalities.

CONCLUSIONS AND PERSPECTIVES

In this account, we have discussed how to approach heterogeneous catalysis using molecular principles. Control of surface silanol density is one approach that we have used to site isolate inorganic complexes on surfaces. This general strategy is particularly useful for grafting homoleptic organometallic complexes on silica, though tactics to install neutral ligands on dehydroxylated silica surfaces are currently unavailable. Using sol−gel techniques, we can control the overall functional group site density on a silica surface, which allows us to engineer metal binding fragments that can mimic the behavior of homogeneous catalysts. All of the cases discussed here show activities similar to the homogeneous analogues, and in a few cases, we have developed materials that are more active and/or stable. This technique generates materials with predictable properties that are characterized using solid-state NMR. The long experimental acquisition time commonly encountered in this class of materials has recently been alleviated with the introduction of DNP SENS, which dramatically reduces experiment time.

We believe this method of material synthesis and DNP SENS could be generally applied to other catalytic systems, and its use will allow for the construction of quantitative structure−activity relationships that will ultimately lead to better catalyst activities and stabilities. For example, catalysts with predefined domains for different reactions can improve the efficiency of multistep reactions for fine chemicals that are amenable to DNP SENS.[93,94] Similarly, periodic mesoporous organosilicas (PMO)[95,96] were developed and found to be very promising catalysts.[97,98] We should note that PMO materials are also compatible with DNP SENS.[99] Polyoxometalates[100] offer yet another possibility to install molecular level definition in heterogeneous catalysts. Taken together, these seemingly disparate classes of materials

Scheme 9. (a) Semi-Hydrogenation of Alkynes. (b) Homogeneous Analogue of Mat-Pd. (c) Scope, TOF, TON, and Selectivity of the Semi-Hydrogenation of Alkynes

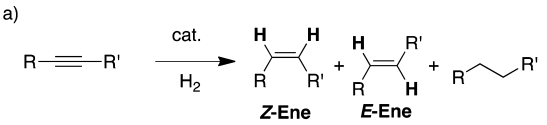

c)

Catalyst	Substrate	TOF (h^{-1})	TON	*Z*-Ene Selectivity 50 % Conv.	*Z*-Ene Selectivity >99 % Conv.
Mat-Pd	Ph—≡—Me **Yne-1**	1800	1100	93	89
20	**Yne-1**	-	*ca.* 100	90	-
Mat-Pd	Ph—≡—Ph **Yne-2**	5100	3100	81	56
Mat-Pd	^{n}Hex—≡—H **Yne-3**	1200	2200	94	85
Mat-Pd	^{n}Pr—≡—^{n}Pr **Yne-4**	13200	3300	94	92
Mat-Pd	OH —≡—(CH2)3 **Yne-5**	4500	2100	93	87

dx.doi.org/10.1021/cs500262t | *ACS Catal.* 2014, 4, 1458−1469

can all provide catalysts for quantitative structure−activity relationships that are generally elusive with classical heterogeneous catalysts.

AUTHOR INFORMATION

Corresponding Authors

*E-mail: (C.C.) ccoperet@inorg.chem.ethz.ch.
*E-mail: (C.T.) thieuleux@cpe.fr.

Notes

The authors declare no competing financial interest.

REFERENCES

(1) *Synthesis Of Solid Catalysts*; de Jong, K. P., Ed.; Wiley−VCH: Weinheim, 2009.
(2) Ballard, D. G. H. In *Adv. Catal.*; Eley, D. D., Pines, H., Veisz, P. B., Eds.; Academic Press: New York, 1973; Vol. *23*, pp 263−325.
(3) Yermakov, Y. I. In *Studies in Surface Science and Catalysis*; Seivama, T., Tanabe, K., Eds.; Elsevier: New York, 1981; Vol. *7*, Part A, pp 57−76.
(4) Basset, J. M.; Choplin, A. *J. Mol. Catal.* **1993**, *21*, 95−108.
(5) Guzman, J.; Gates, B. C. *Dalton Trans.* **2003**, 3303−3318.
(6) Copéret, C.; Chabanas, M.; Petroff Saint-Arroman, R.; Basset, J.-M. *Angew. Chem., Int. Ed.* **2003**, *42*, 156−181.
(7) Thomas, J. M.; Raja, R.; Lewis, D. W. *Angew. Chem., Int. Ed.* **2005**, *44*, 6456−6482.
(8) Tada, M.; Iwasawa, Y. *Coord. Chem. Rev.* **2007**, *251*, 2702−2716.
(9) (a) Wegener, S. L.; Marks, T. J.; Stair, P. C. *Acc. Chem. Res.* **2011**, *45*, 206−214. (b) Conley, M. P.; Delley, M. F.; Siddiqi, G.; Lapadula, G.; Norsic, S.; Monteil, V.; Safonova, O. V.; Copéret, C. *Angew. Chem. Int. Ed.* **2014**, *53*, 1872−1876.
(10) Rascon, F.; Wischert, R.; Copéret, C. *Chem. Sci.* **2011**, *2*, 1449−1456.
(11) Basset, J. M.; Candy, J.-P.; Copéret, C. In *Comprehensive Organometallic Chemistry: From Fundamentals to Applications*; Crabtree, R., Mingos, M., Eds.; Elsevier: New York, 2006.
(12) Liang, Y.; Anwander, R. *Dalton Transactions* **2013**, *42*, 12521−12545.
(13) Chabanas, M.; Baudouin, A.; Copéret, C.; Basset, J.-M. *J. Am. Chem. Soc.* **2001**, *123*, 2062−2063.
(14) Copéret, C. *Dalton Trans.* **2007**, 5498−5504.
(15) Popoff, N.; Mazoyer, E.; Pelletier, J.; Gauvin, R. M.; Taoufik, M. *Chem. Soc. Rev.* **2013**, *42*, 9035−9054.
(16) Vidal, V. V.; Theolier, A.; Thivolle-Cazat, J.; Basset, J.-M. *Science* **1997**, *276*, 99−102.
(17) Copéret, C.; Maury, O.; Thivolle-Cazat, J.; Basset, J.-M. *Angew. Chem., Int. Ed.* **2001**, *40*, 2331−2334.
(18) Blanc, F.; Copéret, C.; Thivolle-Cazat, J.; Basset, J.-M. *Angew. Chem., Int. Ed.* **2006**, *45*, 6201−6203.
(19) Thieuleux, C.; Maraval, A.; Veyre, L.; Copéret, C.; Soulivong, D.; Basset, J.-M.; Sunley, G. J. *Angew. Chem., Int. Ed.* **2007**, *46*, 2288−2290.
(20) Basset, J.-M.; Copéret, C.; Soulivong, D.; Taoufik, M.; Cazat, J. T. *Acc. Chem. Res.* **2010**, *43*, 323−334.
(21) Copéret, C. *Chem. Rev.* **2010**, *110*, 656−680.
(22) Gajan, D.; Copéret, C. *New J. Chem.* **2011**, *35*, 2403−2408.
(23) Ruddy, D. A.; Jarupatrakorn, J.; Rioux, R. M.; Miller, J. T.; McMurdo, M. J.; McBee, J. L.; Tupper, K. A.; Tilley, T. D. *Chem. Mater.* **2008**, *20*, 6517−6527.
(24) Clearfield, A. *Chem. Mater.* **1998**, *10*, 2801−2810.
(25) Moller, K.; Bein, T. *Chem. Mater.* **1998**, *10*, 2950−2963.
(26) Stein, A.; Melde, B. J.; Schroden, R. C. *Adv. Mater.* **2000**, *12*, 1403−1419.
(27) Cauvel, A.; Renard, G.; Brunel, D. *J. Org. Chem.* **1997**, *62*, 749−751.
(28) Mercier, L.; Pinnavaia, T. J. *Adv. Mater.* **1997**, *9*, 500−503.
(29) Corriu, R. J. P.; Mehdi, A.; Reye, C. *J. Mater. Chem.* **2005**, *15*, 4285−4294.
(30) Hoffmann, F.; Cornelius, M.; Morell, J.; Fröba, M. *J. Nanosci. Nanotechnol.* **2006**, *6*, 265−288.
(31) Diaz, U.; Brunel, D.; Corma, A. *Chem. Soc. Rev.* **2013**, *42*, 4083−4097.
(32) Hoffmann, F.; Cornelius, M.; Morell, J.; Fröba, M. *Angew. Chem., Int. Ed.* **2006**, *45*, 3216−3251.
(33) Schuth, F. *Angew. Chem., Int. Ed.* **2003**, *42*, 3604−3622.
(34) Boullanger, A.; Alauzun, J.; Mehdi, A.; Reye, C.; Corriu, R. J. P. *New J. Chem.* **2010**, *34*, 738−743.
(35) Lelli, M.; Gajan, D.; Lesage, A.; Caporini, M. A.; Vitzthum, V.; Miéville, P.; Héroguel, F.; Rascon, F.; Roussey, A.; Thieuleux, C.; Boualleg, M.; Veyre, L.; Bodenhausen, G.; Copéret, C.; Emsley, L. *J. Am. Chem. Soc.* **2011**, *133*, 2104−2107.
(36) Lim, M. H.; Stein, A. *Chem. Mater.* **1999**, *11*, 3285−3295.
(37) Yokoi, T.; Yoshitake, H.; Tatsumi, T. *J. Mater. Chem.* **2004**, *14*, 951−957.
(38) Mouawia, R.; Mehdi, A.; Reye, C.; Corriu, R. J. P. *J. Mater. Chem.* **2008**, *18*, 4193−4203.
(39) Nakazawa, J.; Stack, T. D. P. *J. Am. Chem. Soc.* **2008**, *130*, 14360−14361.
(40) Zagdoun, A.; Casano, G.; Ouari, O.; Lapadula, G.; Rossini, A. J.; Lelli, M.; Baffert, M.; Gajan, D.; Veyre, L.; Maas, W. E.; Rosay, M.; Weber, R. T.; Thieuleux, C.; Copéret, C.; Lesage, A.; Tordo, P.; Emsley, L. *J. Am. Chem. Soc.* **2011**, *134*, 2284−2291.
(41) Gajan, D.; Schwarzwälder, M.; Conley, M. P.; Grüning, W. R.; Rossini, A. J.; Zagdoun, A.; Lelli, M.; Yulikov, M.; Jeschke, G.; Sauvée, C.; Ouari, O.; Tordo, P.; Veyre, L.; Lesage, A.; Thieuleux, C.; Emsley, L.; Copéret, C. *J. Am. Chem. Soc.* **2013**, *135*, 15459−15466.
(42) Huh, S.; Wiench, J. W.; Yoo, J.-C.; Pruski, M.; Lin, V. S. Y. *Chem. Mater.* **2003**, *15*, 4247−4256.
(43) Gartmann, N.; Brühwiler, D. *Angew. Chem., Int. Ed.* **2009**, *48*, 6354−6356.
(44) Sharifi, M.; Marschall, R.; Wilhelm, M.; Wallacher, D.; Wark, M. *Langmuir* **2011**, *27*, 5516−5522.
(45) Nakazawa, J.; Smith, B. J.; Stack, T. D. P. *J. Am. Chem. Soc.* **2012**, *134*, 2750−2759.
(46) Wessig, M.; Drescher, M.; Polarz, S. *J. Phys. Chem. C* **2013**, *117*, 2805−2816.
(47) Bass, J. D.; Anderson, S. L.; Katz, A. *Angew. Chem., Int. Ed.* **2003**, *42*, 5219−5222.
(48) Mbaraka, I. K.; Radu, D. R.; Lin, V. S. Y.; Shanks, B. H. *J. Catal.* **2003**, *219*, 329−336.
(49) Gonzalez-Arellano, C.; Corma, A.; Iglesias, M.; Sanchez, F. *Chem. Commun.* **2005**, 3451−3453.
(50) Mbaraka, I. K.; Shanks, B. H. *J. Catal.* **2005**, *229*, 365−373.
(51) Clark, J. H.; Macquarrie, D. J.; Tavener, S. J. *Dalton Trans.* **2006**, 4297−4309.
(52) Margelefsky, E. L.; Zeidan, R. K.; Davis, M. E. *Chem. Soc. Rev.* **2008**, *37*, 1118−1126.
(53) Brunelli, N. A.; Venkatasubbaiah, K.; Jones, C. W. *Chem. Mater.* **2012**, *24*, 2433−2442.
(54) Dufaud, V.; Beauchesne, F.; Bonneviot, L. *Angew. Chem., Int. Ed.* **2005**, *44*, 3475−3477.
(55) Corma, A.; Garcia, H. *Adv. Synth. Catal.* **2006**, *348*, 1391−1412.
(56) Elias, X.; Pleixats, R.; Man, M. W. C.; Moreau, J. J. E. *Adv. Synth. Catal.* **2006**, *348*, 751−762.
(57) Elias, X.; Pleixats, R.; Man, M. W. C.; Moreau, J. J. E. *Adv. Synth. Catal.* **2007**, *349*, 1701−1713.
(58) Sommer, W. J.; Weck, M. *Coord. Chem. Rev.* **2007**, *251*, 860−873.
(59) Diez-Gonzalez, S.; Marion, N.; Nolan, S. P. *Chem. Rev.* **2009**, *109*, 3612−3676.
(60) Alauzun, J.; Mehdi, A.; Reye, C.; Corriu, R. *New J. Chem.* **2007**, *31*, 911−915.
(61) Maishal, T. K.; Alauzun, J.; Basset, J.-M.; Copéret, C.; Corriu, R. J. P.; Jeanneau, E.; Mehdi, A.; Reyé, C.; Veyre, L.; Thieuleux, C. *Angew. Chem., Int. Ed.* **2008**, *47*, 8654−8656.
(62) Karamé, I.; Boualleg, M.; Camus, J.-M.; Maishal, T. K.; Alauzun, J.; Basset, J.-M.; Copéret, C.; Corriu, R. J. P.; Jeanneau, E.; Mehdi, A.; Reyé, C.; Veyre, L.; Thieuleux, C. *Chem.—Eur. J.* **2009**, *15*, 11820−11823.

(63) Samantaray, M. K.; Alauzun, J.; Gajan, D.; Kavitake, S.; Mehdi, A.; Veyre, L.; Lelli, M.; Lesage, A.; Emsley, L.; Copéret, C.; Thieuleux, C. *J. Am. Chem. Soc.* **2013**, *135*, 3193−3199.
(64) Reisinger, A.; Trapp, N.; Krossing, I. *Organometallics* **2007**, *26*, 2096−2105.
(65) Baffert, M.; Maishal, T. K.; Mathey, L.; Copéret, C.; Thieuleux, C. *ChemSusChem* **2011**, *4*, 1762−1765.
(66) Conley, M. P.; Drost, R. M.; Baffert, M.; Gajan, D.; Elsevier, C.; Franks, W. T.; Oschkinat, H.; Veyre, L.; Zagdoun, A.; Rossini, A.; Lelli, M.; Lesage, A.; Casano, G.; Ouari, O.; Tordo, P.; Emsley, L.; Copéret, C.; Thieuleux, C. *Chem.—Eur. J.* **2013**, *19*, 12234−12238.
(67) Bilhou, J. L.; Basset, J. M.; Mutin, R.; Graydon, W. F. *J. Am. Chem. Soc.* **1977**, *99*, 4083−4090.
(68) Copéret, C. *Beilstein J. Org. Chem.* **2011**, *7*, 13−21.
(69) Rossini, A. J.; Zagdoun, A.; Lelli, M.; Lesage, A.; Copéret, C.; Emsley, L. *Acc. Chem. Res.* **2013**, *46*, 1942−1951.
(70) Becerra, L. R.; Gerfen, G. J.; Temkin, R. J.; Singel, D. J.; Griffin, R. G. *Phys. Rev. Lett.* **1993**, *71*, 3561−3564.
(71) Rosay, M.; Tometich, L.; Pawsey, S.; Bader, R.; Schauwecker, R.; Blank, M.; Borchard, P. M.; Cauffman, S. R.; Felch, K. L.; Weber, R. T.; Temkin, R. J.; Griffin, R. G.; Maas, W. E. *Phys. Chem. Chem. Phys.* **2010**, *12*, 5850−5860.
(72) Lesage, A.; Lelli, M.; Gajan, D.; Caporini, M. A.; Vitzthum, V.; Miéville, P.; Alauzun, J.; Roussey, A.; Thieuleux, C.; Mehdi, A.; Bodenhausen, G.; Copéret, C.; Emsley, L. *J. Am. Chem. Soc.* **2010**, *132*, 15459−15461.
(73) Zagdoun, A.; Casano, G.; Ouari, O.; Schwarzwälder, M.; Rossini, A. J.; Aussenac, F.; Yulikov, M.; Jeschke, G.; Copéret, C.; Lesage, A.; Tordo, P.; Emsley, L. *J. Am. Chem. Soc.* **2013**, *135*, 12790−12797.
(74) Ni, Q. Z.; Daviso, E.; Can, T. V.; Markhasin, E.; Jawla, S. K.; Swager, T. M.; Temkin, R. J.; Herzfeld, J.; Griffin, R. G. *Acc. Chem. Res.* **2013**, *46*, 1933−1941.
(75) Song, C.; Hu, K.-N.; Joo, C.-G.; Swager, T. M.; Griffin, R. G. *J. Am. Chem. Soc.* **2006**, *128*, 11385−11390.
(76) Blanc, F.; Copéret, C.; Lesage, A.; Emsley, L. *Chem. Soc. Rev.* **2008**, *37*, 518−526.
(77) Lesage, A. *Phys. Chem. Chem. Phys.* **2009**, *11*, 6876−6891.
(78) Zagdoun, A.; Rossini, A. J.; Conley, M. P.; Grüning, W. R.; Schwarzwälder, M.; Lelli, M.; Franks, W. T.; Oschkinat, H.; Copéret, C.; Emsley, L.; Lesage, A. *Angew. Chem., Int. Ed.* **2013**, *52*, 1222−1225.
(79) Zagdoun, A.; Rossini, A. J.; Gajan, D.; Bourdolle, A.; Ouari, O.; Rosay, M.; Maas, W. E.; Tordo, P.; Lelli, M.; Emsley, L.; Lesage, A.; Copéret, C. *Chem. Commun.* **2012**, *48*, 654−656.
(80) Corberan, R.; Sanau, M.; Peris, E. *Organometallics* **2006**, *25*, 4002−4008.
(81) Corberan, R.; Sanau, M.; Peris, E. *J. Am. Chem. Soc.* **2006**, *128*, 3974−3979.
(82) Maishal, T. K.; Boualleg, M.; Bouhrara, M.; Copéret, C.; Jeanneau, E.; Veyre, L.; Thieuleux, C. *Eur. J. Inorg. Chem.* **2010**, *2010*, 5005−5010.
(83) Jessop, P. G.; Ikariya, T.; Noyori, R. *Nature* **1994**, *368*, 231−233.
(84) Jessop, P. G.; Hsiao, Y.; Ikariya, T.; Noyori, R. *Chem. Commun.* **1995**, 707−708.
(85) (a) Filonenko, G. A.; Conley, M. P.; Copéret, C.; Lutz, M.; Hensen, E. J. M.; Pidko, E. A. *ACS Catal.* **2013**, *3*, 2522−2526. (b) Huff, C. A.; Sanford, M. S. *ACS Catal.* **2013**, *3*, 2412−2416.
(86) Jessop, P. G.; Hsiao, Y.; Ikariya, T.; Noyori, R. *J. Am. Chem. Soc.* **1994**, *116*, 8851−8852.
(87) Zhang, Y.; Fei, J.; Yu, Y.; Zheng, X. *Catal. Comm.* **2004**, *5*, 643−646.
(88) Rohr, M.; Günther, M.; Jutz, F.; Grunwaldt, J.-D.; Emerich, H.; Beek, W. v.; Baiker, A. *App. Catal. A.* **2005**, *296*, 238−250.
(89) Schmid, L.; Canonica, A.; Baiker, A. *App. Catal. A.* **2003**, *255*, 23−33.
(90) Phan, N. T. S.; Van Der Sluys, M.; Jones, C. W. *Adv. Synth. Catal.* **2006**, *348*, 609−679.
(91) Weck, M.; Jones, C. W. *Inorg. Chem.* **2007**, *46*, 1865−1875.
(92) Sprengers, J. W.; Wassenaar, J.; Clement, N. D.; Cavell, K. J.; Elsevier, C. J. *Angew. Chem., Int. Ed.* **2005**, *44*, 2026−2029.
(93) Climent, M. J.; Corma, A.; Iborra, S. *Chem. Rev.* **2010**, *111*, 1072−1133.
(94) Garcia-Garcia, P.; Zagdoun, A.; Copéret, C.; Lesage, A.; Diaz, U.; Corma, A. *Chem. Sci.* **2013**, *4*, 2006−2012.
(95) Asefa, T.; MacLachlan, M. J.; Coombs, N.; Ozin, G. A. *Nature* **1999**, *402*, 867−871.
(96) Inagaki, S.; Guan, S.; Ohsuna, T.; Terasaki, O. *Nature* **2002**, *416*, 304−307.
(97) (a) Corma, A.; Das, D.; Garcia, H.; Leyva, A. *J. Catal.* **2005**, *229*, 322−710. (b) Baleizao, C.; Gigante, B. r.; Das, D.; Alvaro, M.; Garcia, H.; Corma, A. *J. Catal.* **2004**, *223*, 106−113.
(98) (a) Waki, M.; Maegawa, Y.; Hara, K.; Goto, Y.; Shirai, S.; Yamada, Y.; Mizoshita, N.; Tani, T.; Chun, W.-J.; Muratsugu, S.; Tada, M.; Fukuoka, A.; Inagaki, S. *J. Am. Chem. Soc.* **2014**, *136*, 4003−4011. (b) Grüning, W. R.; Siddiqi, G.; Safonova, O. V.; Copéret, C. *Adv. Synth. Catal.* **2014**, *356*, 673−679.
(99) Gruning, W. R.; Rossini, A. J.; Zagdoun, A.; Gajan, D.; Lesage, A.; Emsley, L.; Copéret, C. *Phys. Chem. Chem. Phys.* **2013**, *15*, 13270−13274.
(100) (a) Corma, A.; Iborra, S.; Xamena, F.; Monton, R.; Calvino, J. J.; Prestipino, C. *J. Phys. Chem. C* **2010**, *114*, 8828−8836. (b) Sun, M.; Zhang, J.; Putaj, P.; Caps, V.; Lefebvre, F.; Pelletier, J.; Basset, J.-M. *Chem. Rev.* **2014**, *114*, 981−1019.